J. Fluid Mech. (1994), *vol.* 259, *pp.* 149–165

Cavity collapse in a liquid with solid particles

By N. K. BOURNE AND J. E. FIELD
Cavendish Laboratory, Madingley Road, Cambridge, CB3 0HE, UK

(Received 7 May 1993 and in revised form 26 July 1993)

An experimental study of the interaction of weak shock waves in a liquid with bubbles and solid particles has been conducted. Cavities were punched, and solid particles were cast, into a thin sheet of gelatine clamped between two transparent blocks. A shock of pressure 0.3 GPa was introduced by impacting the gelatine layer with a flyer plate. The subsequent collapse of the cavities was photographed using high-speed framing cameras, and waves in the gelatine were visualized using schlieren optics. Assorted cavity/particle geometries were studied. In the first, cavity and particle were aligned on an axis parallel to the incident shock front. The jet crossing the cavity was found to deviate from the perpendicular to the shock front. This deviation was towards the solid particle when separations were small and away from the particle when separations were increased. When a cavity was placed upstream of a solid particle the collapse time was reduced. Conversely, when a cavity was placed downstream of a solid particle, collapse time was increased and the closure was more symmetrical. These observations were explained in terms of wave reflections. Collapses where the cavity/particle axis was inclined to the incident shock showed features of each of the geometries described above.

1. Introduction

In a previous paper (Bourne & Field 1992) we have described the collapse of an isolated cylindrical cavity when a shock wave is incident upon it. The collapse is asymmetric, in contrast with the classical symmetric collapse described by Rayleigh (1917) for an isolated cavity in an infinite liquid. In asymmetric collapse the pressure field across the cavity is non-uniform and in the case of collapse by a shock wave only one half of the cavity sees a pressure pulse. The upstream cavity wall is involuted to form a high-speed liquid jet which crosses the cavity and impacts at the downstream wall. The jet is directed perpendicular to the collapse shock front and on impact creates a localized region of high pressure in the liquid adjacent to the impact point sending a shock wave into the surrounding fluid. The gas trapped within the cavity is rapidly compressed into two isolated lobes in which temperatures may be sufficiently elevated that luminescence is observed. The jet formation process in shock-induced collapses is spallation and does not follow from asymmetry in the velocity potential around the cavity boundary (as in Plesset & Chapman 1971).

In the majority of systems, cavities are generally neither isolated nor found in positions far from solid surfaces. For example, in cavitation there is generally some fluid flow which gives rise to the pressure drops responsible for the fluid 'failing'. This may be driven by a propeller or turbine machinery (Kenn 1970; Avellan & Karimi 1987). In porous compacts of crystalline solids there is adjacent inter-granular space determined by the packing geometry (Taylor 1985). The stimulus for the present work comes from a requirement to understand the initiation of fast reaction in emulsion

explosives. Included air bubbles are present in the emulsion along with hydrophobic aluminium particles, added both to increase the temperature of reaction and to pin the bubbles within the matrix (Bourne 1989; Bourne & Field 1989, 1990). It is not sufficient in such systems to regard cavities as being able to collapse independently without interacting with other inhomogeneities whether they are solid particles or other bubbles. The interactions of collapsing cavities with adjacent particles have been little studied. Bubble–bubble interactions have, however, received some attention.

Bubble–bubble interactions have been studied experimentally using simple geometries of either two or three bubbles. Chaudhri, Almgren & Persson (1982) collapsed closely spaced 6 mm glass balloons suspended in water with a strong shock from a silver azide explosive charge. The glass jets observed within the spheres appeared to deviate away from one another. The results are in accordance with compressive shock reflections (since the bubbles have glass walls) from adjacent collapsing cavities increasing pressure between the cavities and driving the jets to the lower pressure areas. Tomita, Shima & Ohno (1984) isolated several simple geometries in which bubbles were attached to solid surfaces and to pressure transducers. They observed that the jets crossing collapsing 1 mm bubbles adjacent to one another converged towards the axis between the cavities. Testud-Giovanneschi, Alloncle & Dufresne (1990) conducted a similar study with laser-induced bubbles using high-speed streak photography. They observed jet directions, collapse times and measured acoustic wave amplitudes on subsequent rebounds as a function of the number of bubbles present. The bubbles were situated away from free surfaces and their centres were observed to migrate towards one another during collapse. Dear (1985) and Dear & Field (1986, 1988) have presented results in which two-dimensional bubbles placed closely together are collapsed by a 0.3 GPa shock introduced by a flyer plate. They aligned three 3 mm cavities placed with an axis through their centres parallel with the shock front and with adjacent cavity centres 4 mm apart. The jet in the central cavity was observed to cross perpendicular to the shock front. The jets in the outer cavities deviated away from the perpendicular to the shock front on either side. They attributed this to 'compression waves arriving after cavitated regions formed'. A more consistent interpretation was that free surfaces near the outer cavities relieved pressure away from the central region; high pressures in this area then drove the jets towards the free surface (see results below).

Theoretical considerations of the dynamics of cavity clusters and of the interactions of bubbles collapsing near boundaries and free surfaces have been published by Plesset & Chapman (1971), Mørch (1983, 1987), Hansson, Kendrinskii & Mørch (1982), Hansson & Mørch (1980), van Wijngaarden (1972), Blake & Gibson (1987), Blake, Taib & Doherty (1986, 1987). Mørch has shown that cavity clusters form collapse waves with velocities dependent upon the void fraction and incident collapse shock pressure. This approach has been verified by experiment (Bourne & Field 1989, 1992). Blake and his co-workers have produced models which describe the motions of collapsing bubbles adjacent to both free and solid surfaces. They predict jet motion towards solid surfaces and away from free surfaces during collapse, extending the work of Plesset & Chapman.

The following experimental investigation examines the collapse of cavities in proximity to free surfaces, and solid particles and surfaces. The principal investigative tool employed is high-speed framing photography.

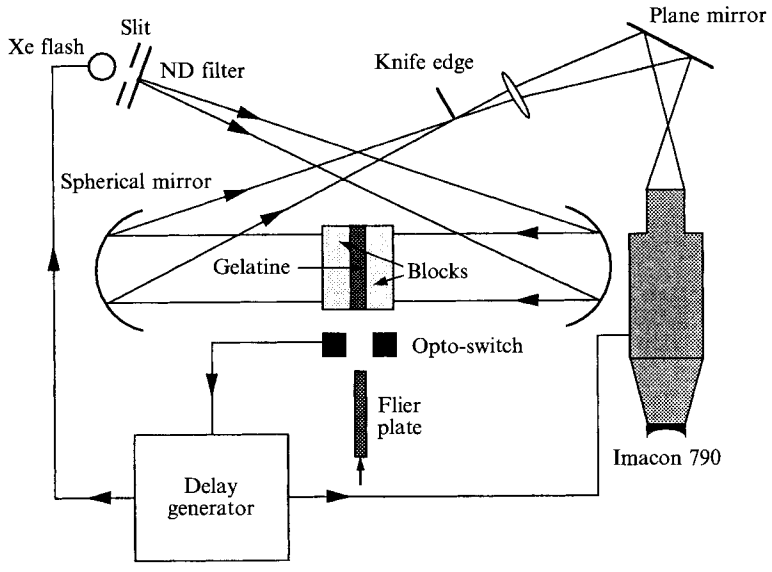

FIGURE 1. Experimental schlieren system employed. The mirrors are of diameter 10.1 cm and of focal length 1.22 m. The diagram is not to scale.

2. Experimental

A method in which liquid-drop impact phenomena might be studied two-dimensionally was suggested by Brunton (1967). He thought that discs might be used to replace drops in rain erosion experiments, and with Camus, designed an apparatus in which a disc of water was held under its own surface tension between two glass blocks and impacted with a metal slider (Brunton & Camus 1970; Camus 1971). The technique was adapted by Dear (1985) to use water with 12% by weight gelatine to give more accurate control over the geometry impacted (Dear & Field 1988; Field, Lesser & Dear 1985). Dear employed the method to look at a few simple cavity collapse configurations (Dear 1985; Dear & Field 1988).

The advantage of studying bubble collapse two-dimensionally is that details of processes occurring within the bubble can be followed without the refraction problems associated with viewing through a curved wall. The gel layer was cast in a mould from 12% by weight of gelatine in water at room temperature (to give a gel density, $\rho = 970 \pm 50$ kg m^{-3}). The mould faces were lightly greased and covered with a thin plastic film. The gelatine layers produced, with plastic sheets attached, could be kept for several days. Solid lead disks of diameter 3 mm were cast into the sheet as required. Cavities were then produced at the required sites by punching out suitable disks. The gelatine lost its viscoelastic properties, undergoing a phase change when shocked.

Both toughened-glass and polymethylmethacrylate (PMMA) blocks were used to confine the sample. The thickness of the blocks was designed to ensure that no rarefaction reached the shock running in the gelatine until it had passed the areas of interest, for example the cavities. The free surfaces of the gelatine sheet within the blocks were butted against PMMA spacers to prevent rarefactions relieving the shock pressure from the sides.

The shock amplitude was 0.3 GPa produced by the impact of a rectangular, phosphor-bronze flyer plate fired between the transparent blocks so that it impacted the front surface of the gelatine. The slider had a circular section removed to reduce its mass and was fired from a rectangular-bore gas gun (Hutchings, Rochester &

Camus 1977). The slider was accelerated to a velocity of about 150 m s^{-1} and had a mass of 5.5 g.

The shock introduced by the flyer plate was of fast rise time. This pressure was maintained around the cavity until rarefactions or reflected shocks reached the collapse site. It was found, by varying the block thickness, flyer dimensions, and the size of the gelatine sheet, that rarefactions did not effect the jet velocity once the shock had passed and that the jet velocity remained constant even though the driving pressure was removed, consistent with the jet being formed by spallation. Collapses were in all cases complete before rarefactions from the block surfaces arrived at the cavity site to relieve pressures.

The collapses were photographed using Hadland Imacon 790 and 792 cameras operating in framing mode and the framing rates were varied from 2×10^5 to 5×10^6 frames per second. The sample was mounted in a conventional two-mirror schlieren system (figure 1). The flash source was a Xenon QCA5 tube which delivered a stored energy of 150 J in approximately 100 μs. The flash and camera were triggered via the three-channel delay generator by the flyer plate cutting an infra-red beam on exiting the gun barrel.

3. Results

3.1. *Interactions of collapsing cavities with free surfaces*

A cavity of diameter 3 mm was placed 2 mm from a free surface and perpendicular to the direction of shock travel. A 0.3 GPa shock was then introduced into the gelatine sheet by slider impact. Figure 2 shows a shadowgraph sequence of the event. The free surface is visible as a vertical line to the left-hand side of the frames. The cavity contains air. Waves are not visible in the picture but the jet direction can clearly be seen with the collapse driven from the right-hand side. The collapse time is around 20 μs, considerably slower than expected for an equivalent cavity far from any boundaries which is between 10 and 15 μs. The jet velocity is similarly reduced.

3.2. *Transient cavity collapse in the presence of solid particles*

Several cavity/particle geometries are considered with cavities punched adjacent to cylindrical particles cast into the gelatine sheet. The cavities are collapsed by a 0.3 GPa shock introduced by flyer-plate impact. The geometries are presented schematically in figure 3 and are labelled A, B, C, D and E in that figure. The collapse geometries A, B and C are considered separately below since each represents a distinct flow configuration whilst D and E combine aspects of A with C or A with B.

3.2.1. *Axis through cavity and particle parallel to shock front*

Figure 4 shows the collapse of a 3 mm cavity placed adjacent to a 3 mm lead disk cast into the gelatine sheet. The centres of the particle and the disk are 5 mm apart. Inclusion separations measured in this paper are defined as being from centre to centre. The interframe time is 5 μs. In frame 1 the incident shock, S, enters and waves are reflected from both cavity and particle; a rarefaction, T, from the former and a shock from the latter. These waves are illustrated schematically in geometry A of figure 3. The shock, S, is diffracted by the cavity and particle and exits the field of view in frame 3. Behind the shock front an area of pressure lower than ambient develops upstream of the cavity in the region reached by the rarefaction. This area of micro-cavities develops as a darker region in frames 2–4. This region is re-compressed by the reflection from the lead particle and is seen to reduce in size in frames 4–6. As the flow behind the

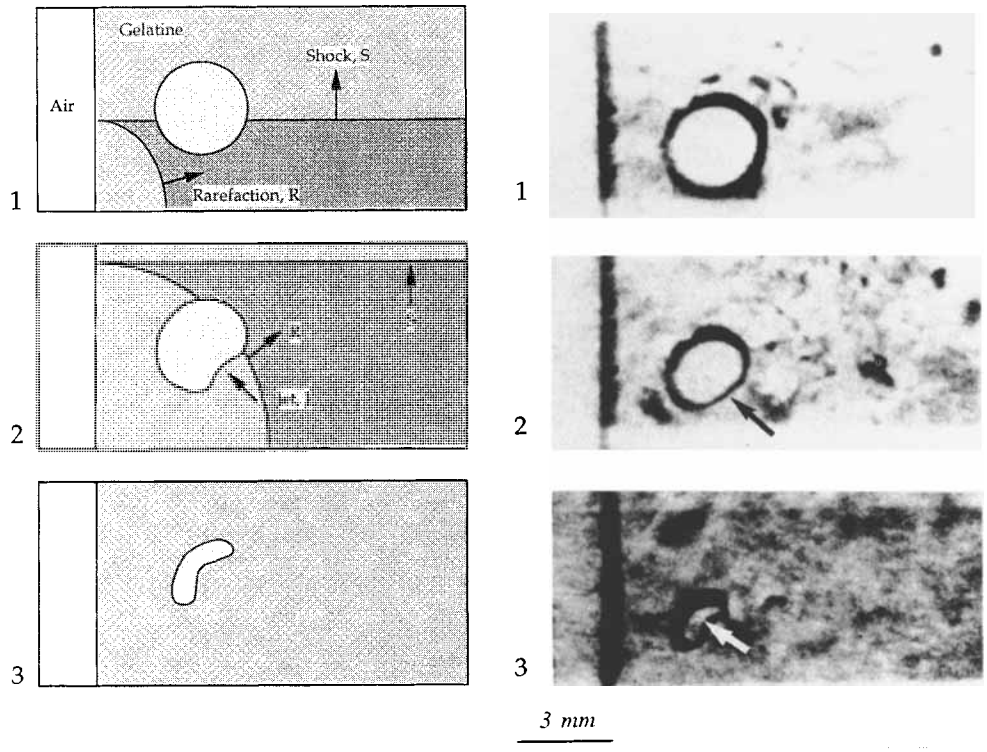

FIGURE 2. The collapse of a 3 mm bubble in proximity to a free surface. The bubble is 2 mm from the surface. The collapsing shock is of magnitude 0.3 GPa. The jet is driven towards the free surface as pressure is relieved on the left of the cavity by rarefactions from the surface. Interframe time 5 μs.

shock (calculated particle velocity 140 m s^{-1}) separates around the lead disk, a stagnation point, P, develops (frames 3 onwards) on the downstream side of the disk. The cavity collapse begins in frame 3 as a jet, J, starts to form on the upstream cavity wall. The jet crosses the cavity and impacts between frames 5 and 6. The cavity collapse time is about 20 μs which is longer than would be expected for a single 3 mm cavity subject to a shock of the same strength. In other work (Bourne & Field 1992) we have shown that an isolated cavity collapses in about 15 μs. The jet impact induces a shock, A, in the fluid, travelling at 1500 m s^{-1}. This shock propagates rapidly from the point of impact but is more easily visible in the region between the particles. This is due to the visualization system used. The jet from the main cavity penetrates the downstream wall to form a pair of counter-rotating vortices which travel downstream in the flow.

The early stages of the interactions for this geometry are shown in figure 5. The particle is again lead and the cavity and particle are placed 12 mm apart. In this case the particle and cavity diameter are 6 mm and each frame has an exposure time of 0.2 μs. The incident shock, S, can be seen travelling upwards in frame 1. It shows slight curvature but this does not account for the position of the forming jet J in frame 3 which is clearly on the right-hand side of the upstream wall. The shock reflection, C, and the rarefaction, T, can be seen in frames 1 and 2 whilst the diffraction of the incident shock is visible in frame 3. By frame 4, 12 μs into the interaction, the jet is deviating away from the solid particle. Again there is an area in which micro-cavities form between the cavity and the particle.

These experiments were repeated varying the particle/cavity separation and the

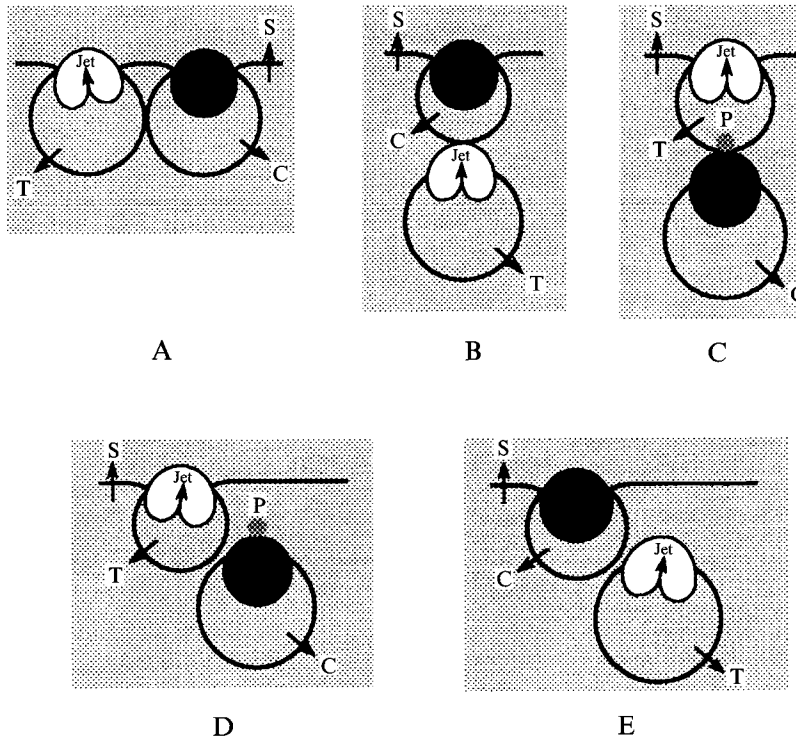

FIGURE 3. A schematic diagram showing the geometries used in the experimental investigation: S, incident shock wave; T, reflected rarefaction wave; C, reflected shock wave.

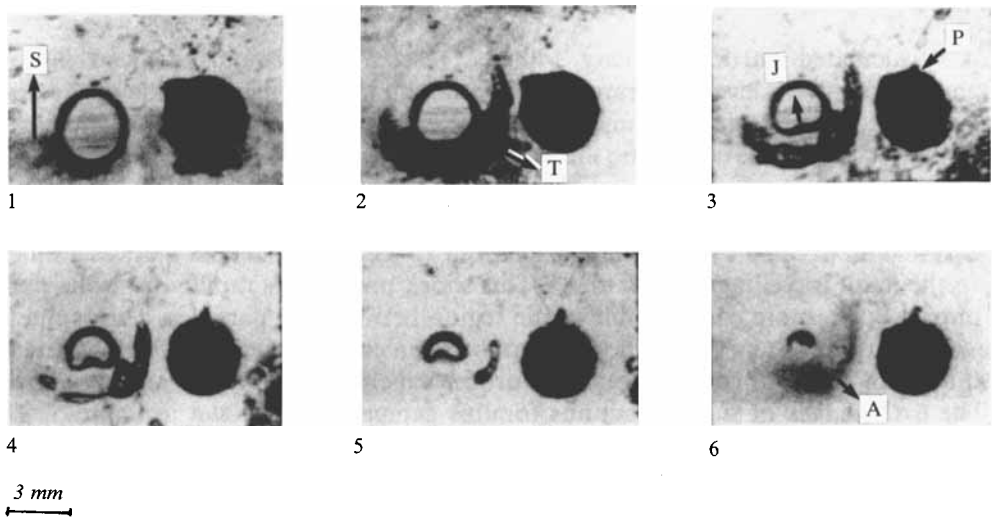

FIGURE 4. Collapse of a 3 mm cavity placed adjacent to a 3 mm lead disk cast into the gelatine sheet when subject to a 0.3 GPa shock. The cavity and particle centres are 5 mm apart. The shock enters in frame 1 and collapse is complete by frame 6. The jet deviates very slightly away from the lead particle. Interframe time is 5 μs.

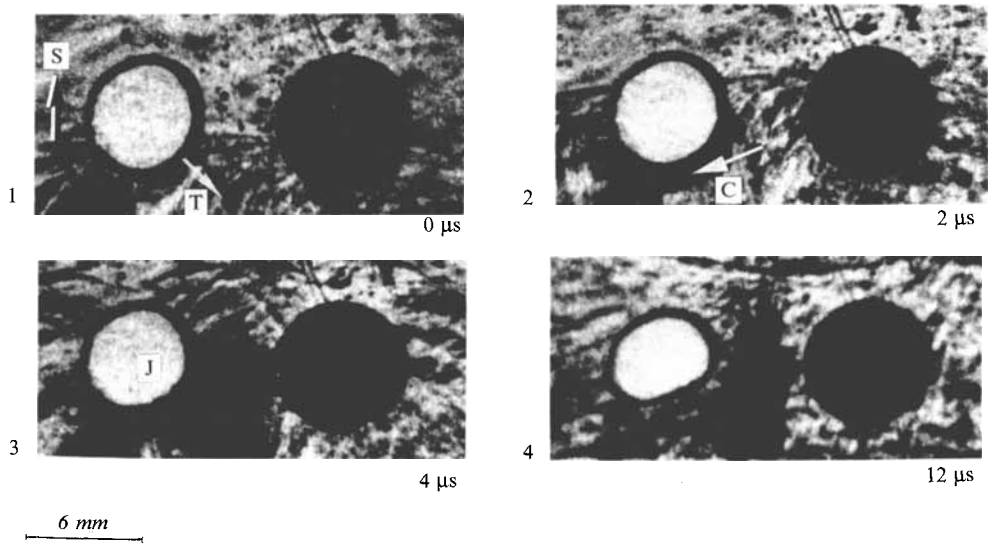

FIGURE 5. The collapse of a 6 mm cavity placed adjacent to a 6 mm lead disk. The cavity/particle separation is 2 diameters (12 mm). The exposure time for each frame is 0.2 μs. The jet formed is deviating away from the particle.

particle material. Figure 6 shows three frames taken from different sequences in which jets are seen crossing cavities and deviating away from and towards the solid inclusions. The only variable in these configurations is the inclusions' separation; the cavity and particle diameter in each case being 3 mm and the shock of amplitude 0.3 GPa. When cavity and particle are close the jets deviate towards the particle in the flow, whilst when the separation increases the jet is driven away from the particle. Collapse times are in all cases above that expected for an isolated cavity.

3.2.2. *Cavity upstream of particle; cavity/particle axis perpendicular to shock front*

In geometry B the cavity is placed directly in front of the particle. In this case the flow field is constrained to be symmetric about an axis between cavity and particle. The direction of jet travel is thus always perpendicular to the shock front. In figure 7 a 3 mm cavity is placed upstream of a 3 mm lead inclusion and collapsed by a 0.3 GPa shock. The incident shock, S, is apparent in frame 1 where it has passed over the particle. A rarefaction wave, T, runs out into the shocked material. Collapse has occurred by frame 3 and the resulting shock, R, can be seen propagating out from the collapse site (which appears as a dark, kidney-shaped area). The incident shock has reflected from the upstream surface of the particle and a compressive wave, C, travels back through the shocked material. Since the particle is sufficiently close to the cavity, this shock reflection acts to drive the downstream wall towards the jet and so speeds the collapse of the cavity. The collapse time is imprecisely determined given the framing rate but is of the order of 5–10 μs, faster than an equivalent isolated cavity. The collapse site, consisting of two counter-rotating vortices, travels downstream (at a speed of about 10 m s^{-1}) through the remaining frames. In frame 7 these vortices part as they travel around the particle. In frame 6 a vortex is shed from the stagnation region at the rear of the particle. The dark object appearing from the bottom in frames 5–10 is the flyer plate used to introduce the shock.

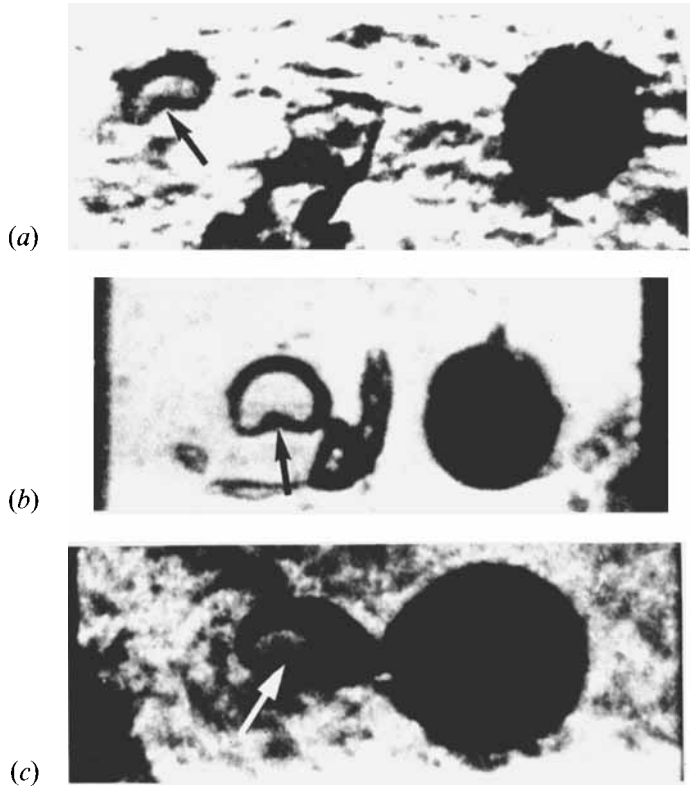

FIGURE 6. Three frames are presented from three sequences illustrating the jet deviations. In (*a*) the separation is large and the compressive reflection dominates the interaction, forcing the jet away from the particle. In (*b*) the jet crosses the cavity without deviation. In (*c*) the flow into the jet is restricted by the presence of the disk. The jet deviates towards the particle. In all cases the particles are lead and of diameter 3 mm.

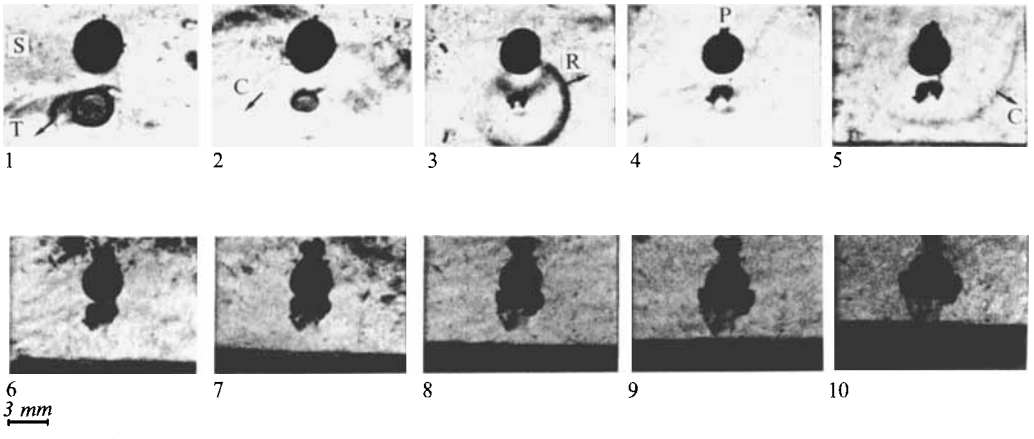

FIGURE 7. A 3 mm cavity upstream of a 3 mm lead particle inclusion on an axis perpendicular to the shock. Note movements of collapse site in the flow up to, and finally around, the particle. Also the vortex, P, shed downstream of the particle. The slider enters the sequence from below in frames 3–5. Interframe time is 5 μs.

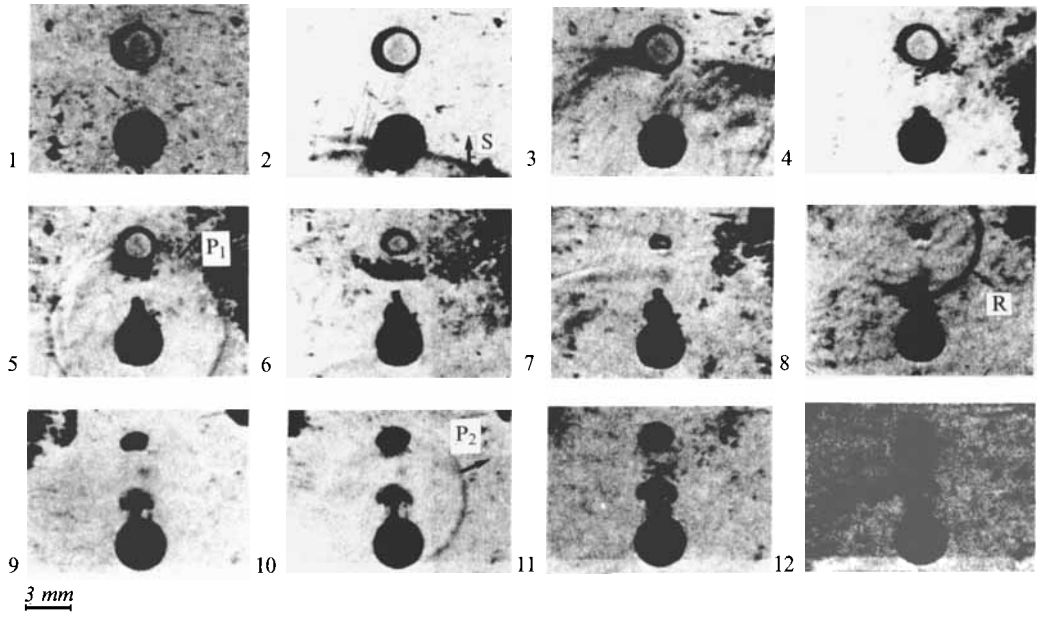

FIGURE 8. Lead particle shielding cavity. Note how much the collapse has slowed down now the cavity is in the shadow zone of the particle. Interframe time is 5 μs. The incident shock is seen entering in frame 2. The collapse finishes in frame 8. The vortices from the stagnation area behind the particle travel downstream in frames 9 onwards. Waves P_1 and P_2 are surface waves associated with vortex formation in the flow around the cylinder.

3.2.3. *Cavity shielded by particle; cavity/particle axis perpendicular to shock front*

In geometry C the particle shields the cavity from the incident shock resulting in an increased collapse time in comparison with B (about 30 μs instead of 15 μs). Figure 8 shows a sequence in which a 3 mm lead disk shields a 3 mm air cavity placed downstream. Frame 1 shows the initial undisturbed geometry before a 0.3 GPa shock, introduced by a flyer plate, enters frame 2 from below. The shocked flow around the particle causes a wake to develop on its downstream side, seen developing from frame 3 onwards. It releases a compressive wave, P_1, centred on this area into the material in frame 5. A rarefaction wave moves into the region between cavity and particle from the upstream cavity wall and lowers pressure here, visible as a dark region of micro-cavitation seen at the cavity wall in frame 5. A jet forms and crosses the cavity, impacting between frames 7 and 8. A shock, R, induced by the jet impact is seen in frame 8. The kidney-shaped collapse site travels downstream through the remaining frames. The vortices shed from the downstream side of the particle in frame 8 also travel with the flow and a further compressive wave, P_2, is released from this region in frame 9.

Figure 9 shows details of the early stages of the flow development. The incident shock, S, has entered in frame 1 and can be seen diffracting around the particle. The reflected shock, C, can also be seen. In frame 3 the head of the rarefaction, T, reflected from the cavity free surface can be seen in the fluid upstream of the cavity. From frame 2 onwards, a dark area is seen developing at the downstream stagnation point of the cylinder. This emits a wave, P_1, starting in frame 4 which propagates outward through frames 5 and 6. There is structure particularly at the left-hand edge of this wave front. The dark, speckled areas seen on the right-hand portion of frame 5 are regions relieved by rarefaction waves from the free gel slab surfaces.

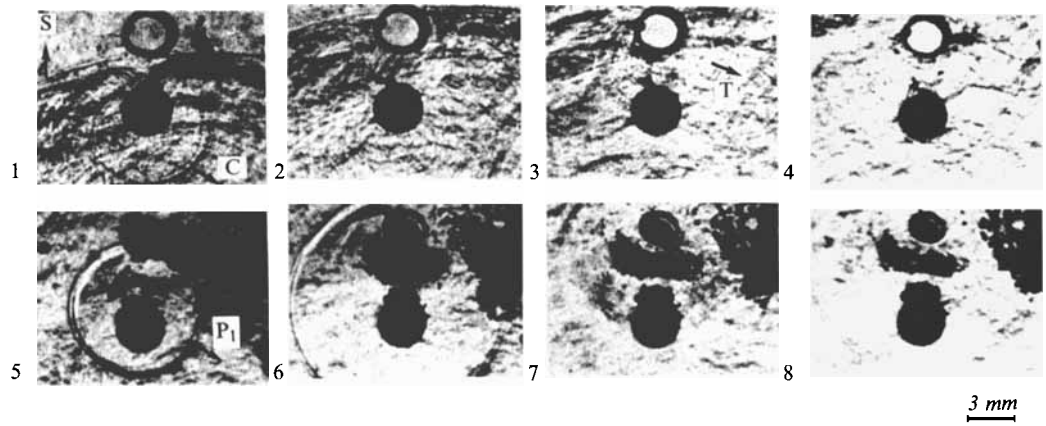

FIGURE 9. The collapse shown in the previous figure is presented at a higher framing rate. The structures behind the shock are apparent. The incident shock, S, and compressive reflection, C, is seen in frame 1 and the rarefaction, T, from the cavity in frame 3. The wave from the stagnation area is seen in frame 5. The exposure time for each frame is 0.2 μs.

The speckled appearance is due to sub-millimetre, three-dimensional cavities formed at the fluid/glass interface. This speckling disappears as the wave P_1 runs across this area. It will also be noticed that this wave is not apparently diffracted by the lead disk as one would expect for a wave running through the fluid sheet. The wave must therefore run at the interface between fluid and confining blocks and be associated with the shedding of vortices from downstream of the particle. Such waves (see also P_2 in figure 8) can be regarded as artefacts of the experimental configuration.

A region of relieved pressure between cavity and particle can be seen as a dark area in frames 6–8 of figure 9. The structure apparent in the picture is an indication of the turbulent nature of the flow behind the shock. It should be noted that the dark areas including the wake and micro-cavitation present in these gelatine experiments have also been observed under the same experimental conditions with tap water replacing gelatine as the fluid.

3.2.4. *Cavity/particle axis inclined to shock front*

Interactions described in the previous sections can be used to predict the behaviour expected from geometries D and E. In geometry D the particle is placed in front of and laterally offset from the cavity; the axis between particle and cavity makes an angle of 45° with the shock front. As in previous experiments the shock strength is 0.3 GPa and the cavity and particle are of diameter 3 mm. The collapse sequence, shown in figure 10, has an interframe time of 5 μs.

The incident shock, S, can be seen in frame 1 as can a reflected shock, C, from the particle. By frame 2 the shock has passed over the cavity and the upstream wall has started to involute to form the jet. A region of relieved pressure can be seen developing upstream of the cavity. In frame 4 the jet, J, can be seen forming and its direction is inclined towards the cavity/particle axis. The flow around the particle forms vortices on the downstream wall which detach with the emission of a surface wave P in frame 4. The cavity finally closes some time after frame 6, giving a collapse time in excess of 20 μs.

In the case of geometry E the particle can only affect the collapse during its final stages since the shock must pass over the cavity first. The sequence is presented in figure

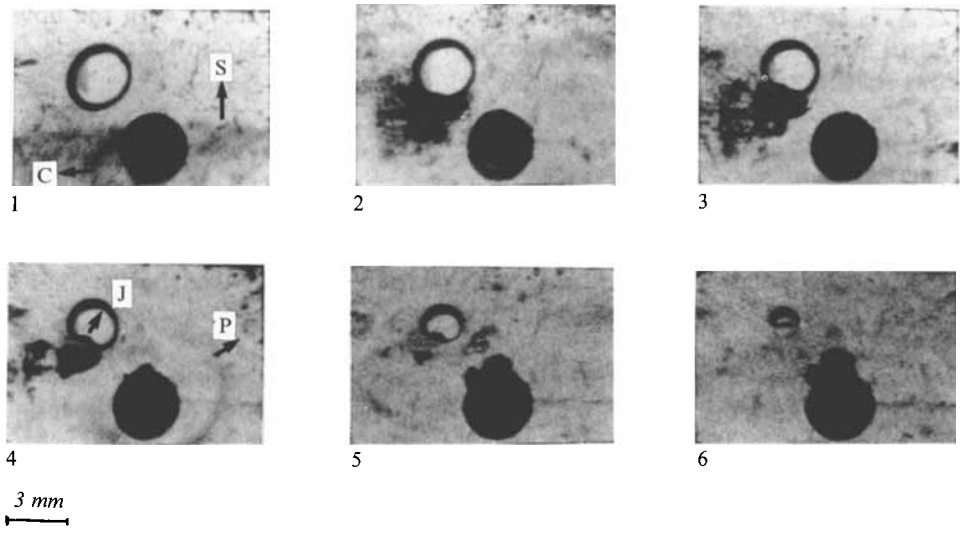

FIGURE 10. The collapse of a cavity after the shock has first passed over a lead particle. The shock pressure is 0.3 GPa. Interframe time is 5 μs. The jet shows deviation towards the axis between particle and cavity.

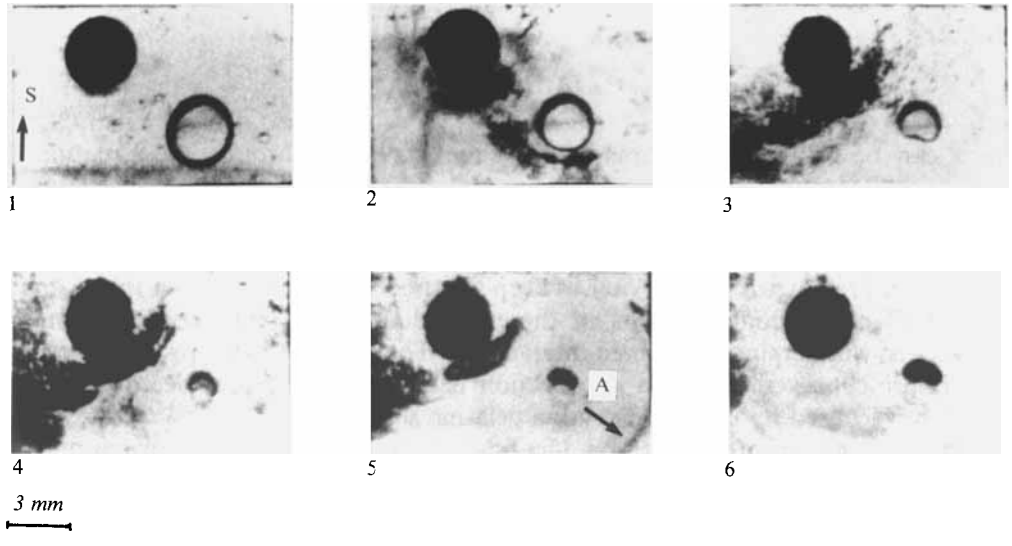

FIGURE 11. The collapse of a 3 mm bubble with the cavity placed ahead of the particle. The collapse is affected less by the presence of the particle than in the previous figure. Note how much the collapse is slowed in the sequence of figure 10 compared with that in this figure.

11 and particle diameters and shock pressures are as above. The incident shock, S, is seen in frame 1 where it encounters the cavity. In frame 2 it can be seen just clearing the particle. A relieved area has developed upstream of the cavity and a dark area indicates a pressure gradient between cavity and particle. The collapse proceeds in frame 2–5 with final jet impact occurring just after frame 4. This gives a collapse time for the cavity of the order of 15 μs, close to that for an isolated cavity (Bourne & Field 1992). The jet deviates slightly away from an axis perpendicular to the shock front. A

shock, A, is seen in frame 5. The collapse site travels downstream with the flow at around 10 m s^{-1}. In later frames (not shown) vortices are shed from the particle as in previous sequences.

4. Discussion

Free or solid surfaces and particles can only influence transient collapses if waves can propagate from one to the other before the collapse is complete. A simple parameter to determine the range of influence of such interactions is derived below. Acoustic approximations are assumed since in these experiments shock velocities are very close to acoustic velocities.

Consider a cavity of diameter D, placed a distance d from a surface of some kind (another cavity, a solid interface, etc.). The jet velocity is given in a one-dimensional approximation by $2v$, which defines a collapse time for the cavity to be

$$\tau = D/2v'. \tag{1}$$

If the reflected shock or release wave is assumed to travel at close to the acoustic velocity, c, in the fluid (as is the case in this work) then it can travel a distance, $c\tau$ during the collapse. If this distance is greater than d then the collapse will be unaffected by the boundary. This maximum distance R_{max} can be expressed as a radius of influence for a perturbing inhomogeneity. Normalizing by the cavity diameter a non-dimensional parameter N_{max} is obtained,

$$N_{max} = \frac{R_{max}}{D} = \frac{c}{2v'} \tag{2}$$

which can be expressed in terms of the shock pressure through the equation of momentum conservation $P = \rho cv$.

Substituting for parameters in the present experiments gives 5 cavity diameters as a maximum radius of influence for an inhomogeneity. Note the reciprocal dependence upon shock pressure. It is thus vital to keep any free boundaries at least this distance away from cavity configurations in these two-dimensional experiments otherwise rarefactions will dominate observed interactions. The jet deviations presented by Dear & Field are consistent with the jet direction being due to the presence of free fluid boundaries (caused by using too small a gelatine slab).

Any cavity placed equidistant from identical inhomogeneities and on an axis parallel to the shock front will experience no jet deviations but altered collapse times due to perturbations in the pressure field driving the jet. Obviously, control of jet direction and velocity in a particular collapsing cavity may be achieved by the positioning of free surfaces in the flow. Solid particles will have analogous effects. Assuming that the reflected shocks are again weak, the above parameter can be used to determine radii of influence.

4.1. *Interactions of collapsing cavities with free surfaces*

The sequence of figure 2 can be explained in terms of the release wave propagating from the free surface behind the incident shock. Pressure will be relieved on the side of the cavity closest to the surface and flow of material into the jet will be principally from the right-hand side. Clearly if the cavity has time to collapse before the release wave can arrive, then the presence of the surface will have no effect.

Tomita *et al.* (1984) have presented work with an essentially equivalent configuration. The cavities interact with one another via the release waves reflected by

	Jet deviation (±5°)	Separation (±0.2 cavity diameters)
Lead	−20	1.0
	10	1.7
	18	2.3
	28	3.1
	15	3.4
Nylon	−10	2.3
	−15	1.7
	−15	2.0
	24	3.3

TABLE 1. Jet deviations for lead and nylon particles. Positive angles represent deviations away from the particle whilst negative angles represent deviations towards the particle.

the incident shock and the jets within the cavities converge since the flow is restricted between the bubbles (or the pressure in that region is reduced which is equivalent). The results of Chaudhri *et al.* (1982) are consistent with compressive reflections from the glass spheres increasing pressure in the region between the cavities. It is apparent that the jet velocities and directions are determined by conditions at the moment of jet formation and not by subsequent pressure fluctuations behind the driven wall of the cavity (unless pressure there can *increase* rapidly). This is a defining feature of shock-induced cavity collapse where jet formation is a spallation phenomenon. Such glass cavities (microballoons) are introduced into emulsion explosives to sensitize these energetic materials to shock. There are thus differing interactions between these glass additives and genuine pore volume with free surfaces within the explosive as is found, for example, in a crystalline compact.

4.2. *Transient cavity collapse in the presence of solid particles*

4.2.1. *Axis through cavity and particle parallel to shock front*

Figures 4–6 illustrate jet deviations when cavities collapse adjacent to solid particles. In each case cavity and particle are of the same diameter. The only variable in these configurations is the cavity/particle separation. When cavity and particle are close the jets deviate towards the particle, whilst when separation increases the jet is driven away from the particle. The magnitude of this deviation has been measured at several separations and the results are presented in table 1. Here the angle through which the jet has deviated from an axis perpendicular to the incident shock front is presented along with the separation between particle and cavity normalized by cavity/particle diameter. Positive angles correspond to deviations away from the particle whilst negative angles correspond to deviations towards it.

Two particle materials were investigated: the lead particles discussed above and nylon particles, chosen as representative of a material with a lower acoustic impedance. For both types of particle close separations cause negative (jet deviates towards particle) deflections. For large separations, jet deviation is positive. At some critical intermediate distance, the jet travels across the cavity unaffected by the presence of the particle. This critical distance is estimated to be 1.5 diameters for lead particles 2.2 diameters for nylon particles.

To account for the observed deflections requires consideration of both the reflected compressive waves from the particle and the effects of the particle itself upon the flow (a Bjerknes interaction). The compressive, shock reflection will tend to increase the

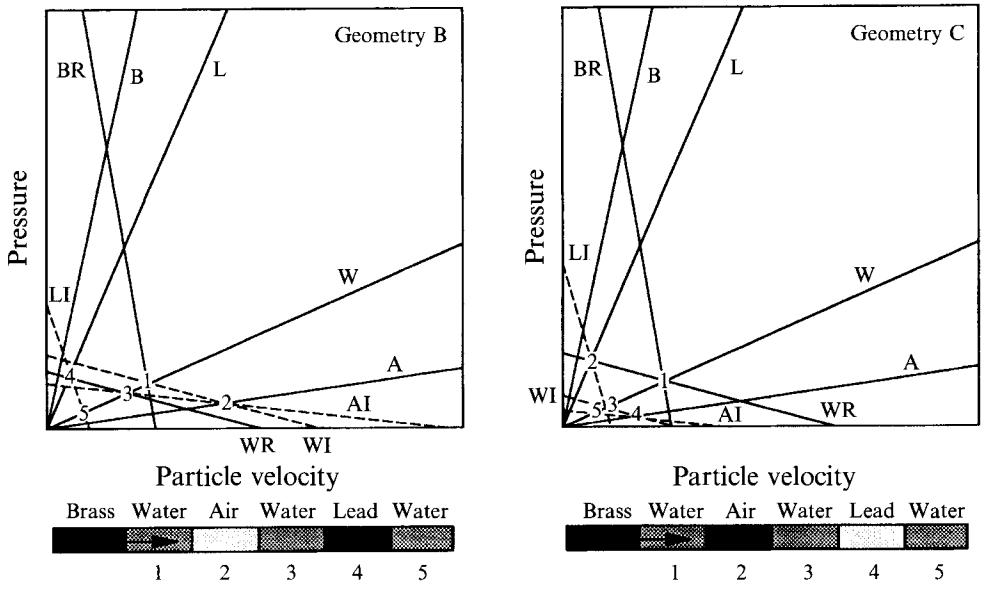

FIGURE 12. Pressure/particle velocity plots and schematics for the one-dimensional models of geometries B and C. The curves are not to scale. The coding for each of the curves is as follows. W, L, A and B are the Hugoniots for water, lead, air and brass. A second letter I signifies an isentrope, whilst a second letter R signifies a reflected shock. The numbers refer to the states in the indicated regions, see table 2.

pressure on the side of the cavity closest to the particle and thus drive the jet away. This effect will be overcome when separations become small since flow into the region between particle and cavity is restricted and the jet is formed by fluid flowing in towards the particle. The jet deviation must thus be composed of two competing interactions. When the acoustic impedance mismatch between the particles and the fluid is large then the amplitude and energy reflection coefficients for the reflected shock will also be large. In these cases the compressive waves will be expected to dominate the interaction and small separations will be required before the geometrical flow effect becomes important. When the mismatch is smaller, the compressive shock will be weaker and the geometrical effects more apparent. This is observed in our data with jet deviation *towards* the particle found over larger distances for the nylon particle than for the lead.

4.2.2. *Cavity/particle axis perpendicular to shock front*

The sequence of figure 7 shows the collapse of a 3 mm cavity placed upstream of a 3 mm lead disk. The collapse time is reduced below that expected for an isolated cavity by the spallation of the downstream cavity wall by the reflected shock from the lead particle. This situation can be contrasted with the sequences of figures 8 and 9 where the collapse time is more than doubled by the shielding of the cavity from the incident shock. A simple one-dimensional model of the wave interactions can be constructed in which the geometries B and C can be represented as plugs of water, air, and lead with a brass plate impacted upon them (shown schematically in figure 12). The various pressures and particle velocities in the different materials (marked in the figure as numbered regions) can be calculated by finding the intersections of relevant Hugoniot, reflected Hugoniot and isentrope curves. The Hugoniots were approximated by polynomial fits to data from Marsh (1980). Fluid states in each region were determined

	Geometry B			Geometry C		
Region	Pressure P (GPa)	Particle velocity u (m s^{-1})	Shock velocity U_s (m s^{-1})	Pressure P (GPa)	Particle velocity u (m s^{-1})	Shock velocity U_s (m s^{-1})
1	0.3	140	1900	0.3	140	1900
2	5×10^{-4}	280	340	0.5	20	2500
3	9×10^{-4}	0.5	1800	0.1	30	1800
4	2×10^{-3}	0.1	2400	1×10^{-4}	70	340
5	2×10^{-4}	0.1	1800	2×10^{-4}	0.1	1600

TABLE 2. Calculated pressures, particle velocities, and wave velocities for the interactions of geometries B and C in a one-dimensional model. The regions referred to are those of figure 12.

from the intersections of equilibrium Hugoniot and isentrope curves in the pressure/particle velocity plane and these are marked in figure 12. Table 2 shows calculated flow variables for the regions defined in the figure.

This model predicts a jet velocity of close to 300 m s^{-1} for the collapse of a cavity placed upstream of a particle, giving a collapse time of 10 μs. Such a collapse time agrees well with the observed behaviour from the photographs. When the shock reflects from the lead particle the pressure in region 3 doubles. This results in the downstream cavity wall being accelerated towards the approaching jet if the reflected shock can reach it before complete closure has occurred. This reduces the collapse time and increases the violence of the collapse as observed.

In contrast, when the cavity is placed downstream of a solid particle the pressure driving the collapse is markedly reduced. This leads to a lowered jet velocity of only 70 m s^{-1} and a consequent collapse time of the order of 45 μs. The observed value of between 20 and 25 μs is a consequence of the diffraction of the shock wave around the particle. The large inertia of the solid particle results in it moving negligibly in the flow on the timescale of the cavity collapse. It will be noticed from the sequence of figure 8 that the micro-jet formed by the involuting upstream cavity wall is less distinct than in cases where the shock waves is incident directly onto the particle. This is a consequence of the lowered pressures in the lee of the particle and a reduced pressure gradient across the cavity.

In both the sequences of geometries B and C there is significant vorticity in the flow. Further, in geometry B the linear vortex system is separated by flow around the solid particle. This results in increased fluid mixing behind the shock. In an energetic liquid, this will have the effect of increasing mass and thermal diffusivities and thus chemical reaction in a material containing pre-existing reaction sites. Leiper, Kirby & Hackett (1985) have observed an increase of reaction rate with voidage in an emulsion explosive. They argue that chaotic motions produced by perturbations due to the presence of other collapse sites increase reaction in the emulsion in the way described.

5. Conclusions

These experiments have investigated the interactions of shock waves with various cavity/particle configurations. The major effects are apparent in reduced collapse times and in the direction taken by the liquid micro-jet in relation to the direction of travel of the incident shock front. The flow also contains increased vorticity and micro-cavitation. There are several competing mechanisms giving rise to these observations.

The principal effect is that of the flow imposed by the passage of the incident shock. Secondly, there are variations in the flow behind the shock produced by the geometrical arrangement of the inclusions. Finally there are reflected waves propagating in the fluid.

The strongest effects are observed when inhomogeneities are placed in close proximity to one another in which case the flow constrictions are maximized and the subsidiary shocks produced by reflection at boundaries have a smaller effect on the subsequent collapse. In this case the acoustic impedance of the inhomogeneity will assume importance. In the case of materials of low acoustic impedance and small impedance mismatch between inhomogeneity and fluid, the compressive reflections will be of lower magnitude since the amplitude or energy reflection coefficient will be small. In the case of large mismatches between particle and fluid, the reflected shocks can dominate the interaction and flow effects only become important when the fluid flow becomes constricted. These effects are apparent as changes in the direction of jet travel across the cavity.

The behaviour expected for solid-walled cavities introduced into the flow as artificial voidage should be contrasted with that observed here for cavities that have free boundaries. In the former case the reflected waves will be shock waves rather than rarefactions and the consequent interactions will differ in nature. The various geometries may also be used to influence collapse times by denying access to the incident shock front and reducing the impulse that the shock might impart to the collapse. In this case the cavity may experience a much lower shock amplitude or even a relatively long-duration compression wave if shielding is efficient. The collapse is much less violent and asymmetries in the collapse become less apparent. Geometry can be used to increase pressure around the collapse site by using the compressive reflections from solid particles. In this case the collapse can be made more violent and collapse times will be reduced.

Regardless of the arrangement of solid particles and cavities the flow following a shock travelling in a fluid with particles is turbulent and contains significant vorticity.

N.K.B. thanks ICI for a CASE studentship and the Royal Commission for the Exhibition of 1851 for a research fellowship for the period over which this work was carried out. SERC is thanked for its support of the high-speed camera studies.

REFERENCES

AVELLAN, F. & KARIMI, A. 1987 Dynamics of vortex cavitation involved in the erosion of hydraulic machines. In *Proc. 7th Intl. Conf. on Erosion by Liquid and Solid Impact* (ed. J. E. Field & J. P. Dear), pp. 25-1–25-7. Cavendish Laboratory, Cambridge, UK.

BLAKE, J. R. & GIBSON, D. C. 1987 Cavitation bubbles near boundaries. *Ann. Rev. Fluid Mech.* **19**, 99–123.

BLAKE, J. R. & TAIB, B. B. & DOHERTY, G. 1986 Transient cavities near boundaries. Part 1. Rigid boundary. *J. Fluid Mech.* **170**, 479–497.

BLAKE, J. R., TAIB, B. B. & DOHERTY, G. 1987 Transient cavities near boundaries. Part 2. Free surface. *J. Fluid Mech.* **181**, 197–212.

BOURNE, N. K. 1989 Shock interactions with cavities. PhD thesis, University of Cambridge.

BOURNE, N. K. & FIELD, J. E. 1989 Cavity collapse in a heterogeneous commercial explosive. In *Proc. Ninth Symp. (Intl.) on Detonation, Portland, Oregon*, pp. 869–878. Office of Naval Research, Washington.

BOURNE, N. K. & FIELD, J. E. 1990 Cavity collapse in reactive and non-reactive media. In *Proc. 19th Intl. Conf. on High-Speed Photography and Photonics, Cambridge, September*, pp. 1046–1056. Soc. Photo Optical Instrumentation Engrs, 1358, Washington.

BOURNE, N. K. & FIELD, J. E. 1992 Shock induced collapse of single cavities in liquids. *J. Fluid Mech.* **244**, 225–240.

BRUNTON, J. H. 1967 Erosion by liquid shock. In *Intl. Conf. Rain Erosion* (ed A. A. Fyall & R. B. King), pp. 821–823. R.A.E. Farnborough, UK.

BRUNTON, J. H. & CAMUS, J.-J. 1970 The application of high-speed photography to analysis of flow in cavitation and drop-impact studies, In *Proc. Intl. Conf. High-Speed Photography* (ed. W. G. Hyzer & W. G. Chase), pp. 444–449. Soc. Motion Picture & Television Engineers, New York.

CAMUS, J.-J. 1971 High-speed flow in impact and its effect on solid surfaces. PhD thesis, University of Cambridge.

CHAUDHRI, M. M., ALMGREN, L.-A. & PERSSON, A. 1982 High-speed photography of the interaction of shocks with voids in condensed media. In *15th Int. Congr. on High-Speed Photography and Photonics, San Diego,* pp. 388–394. Soc. Photo Optical Instrumentation Engrs.

DEAR, J. P. 1985 The fluid mechanics of high-speed impact. PhD thesis, University of Cambridge.

DEAR, J. P. & FIELD, J. E. 1986 A study of the collapse of arrays of cavities using two-dimensional gelatine configurations. In *Proc. Intl. Symp. on Cavitation, Sendai, Japan* (ed. H. Murai), pp. 89–94, Tohoku University.

DEAR, J. P. & FIELD, J. E. 1988 A study of the collapse of arrays of cavities. *J. Fluid Mech.* **190**, 409–425.

FIELD, J. E., LESSER, M. B. & DEAR, J. P. 1985 Studies of two-dimensional liquid wedge impact and their relevance to liquid-drop impact problems. *Proc. R. Soc. Lond.* A **401**, 225–249.

HANSSON, I., KENDRINSKII, V. & MØRCH, K. A. 1982 On the dynamics of cavity clusters. *J. Phys.* D: *Appl. Phys.* **15**, 1725–1734.

HANSSON, I. & MØRCH, K. A. 1980 The dynamics of cavity clusters in ultrasonic (vibratory) cavitation erosion. *J. Appl. Phys.* **51**, 4651–4658.

HUTCHINGS, I. M., ROCHESTER, M. C. & CAMUS, J.-J. 1977 A rectangular bore gas-gun. *J. Phys* E: *Sci. Instrum.* **10**, 455–457.

KENN, M. J. 1983 Cavitation and cavitation damage in concrete structures. *Proc. 6th Intl. Conf. on Erosion by Liquid and Solid Impact* (ed. J. E. Field & N. S. Corney), pp. 12-1 to 12-6. Cavendish Laboratory, Cambridge.

LEIPER, G. A., KIRBY, I. J. & HACKETT, A. 1985 Determination of reaction rates in intermolecular explosives using the electromagnetic particle velocity gauge. In *Proc. Eighth Symp. (Intl.) on Detonation, Albuquerque, New Mexico, July,* pp. 187–195. Office of Naval Research, Washington.

MARSH, S. P. 1980 *LASL Shock Hugoniot data.* University of California Press.

MØRCH, K. A. 1983 Fundamental aspects of the dynamics of cavitating liquids. Dr. Techn. thesis, Technical University of Denmark.

MØRCH, K. A. 1987 The structure of cavity clusters and their damage capability. In *Proc. 7th Intl Conf. on Erosion by Liquid and Solid Impact* (ed. J. E. Field & J. P. Dear), pp. 26-1–26-6. Cavendish Laboratory, Cambridge.

PLESSET, M. S. & CHAPMAN, R. B. 1971 Collapse of an initially spherical vapour cavity in the neighbourhood of a solid boundary. *J. Fluid Mech.* **47**, 283–290.

RAYLEIGH, LORD 1917 On the pressure developed during the collapse of a spherical cavity. *Phil. Mag.* **34**, 94–98.

TAYLOR, P. A. 1985 The effects of material microstructure on the shock-sensitivity of porous granular explosives. In *Proc. Eighth Symp. (Intl.) on Detonation, Albuquerque, New Mexico, July,* pp. 26–33. Office of Naval Research, Washington.

TESTUD-GIOVANNESCHI, P., ALLONCLE, A. P. & DUFRESNE, D. 1990 Collective effects of cavitation: Experimental study of bubble-bubble and bubble-shock waves interactions. *J. Appl. Phys.* **67**, 3560–3564.

TOMITA, Y., SHIMA, A. & OHNO, T. 1984 Collapse of multiple gas bubbles by a shock wave and induced impulsive pressures. *J. Appl. Phys.* **56**, 125–131.

WIJNGAARDEN, L. VAN 1972 One-dimensional flow of liquids containing small gas bubbles. *Ann. Rev. Fluid Mech.* **4**, 369–396.